Chemosphere 225 (2019) 53–64

Contents lists available at ScienceDirect

Chemosphere

journal homepage: www.elsevier.com/locate/chemosphere

Multi-spectral characterization of natural organic matter (NOM) from Manitoba surface waters using high performance size exclusion chromatography (HPSEC)

Kenneth Brezinski*, Beata Gorczyca

Department of Civil Engineering, University of Manitoba, Winnipeg, Manitoba, Canada

HIGHLIGHTS

- HPSEC used to partition NOM based on AMW and multi-wavelength absorbance
- UV absorbing moieties traced to DBP formation for 7 Manitoba source waters
- THM formation traced to prominence of select peaks using correlation coefficients
- Contribution of select UV absorbing moieties appears to be halogen specific
- Methodology is not treatment specific to treatment with ion-exchange

GRAPHICAL ABSTRACT

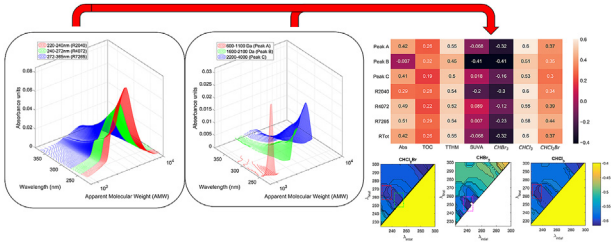

ARTICLE INFO

Article history:
Received 27 October 2018
Received in revised form
24 February 2019
Accepted 25 February 2019
Available online 5 March 2019

Handling Editor: Xiangru Zhang

Keywords:
Ion exchange
Natural organic matter
High performance size exclusion chromatography
Dissolved organic carbon
Trihalomethanes
Disinfection byproducts

ABSTRACT

The main objective of this research was to develop an algorithm that would be able to relate ultraviolet absorbing moieties in potable water to trihalomethanes (THMs) and other water quality parameters. The characterization was carried out using high performance size exclusion chromatography (HPSEC) to separate water samples based on apparent molecule weight (AMW); while the developed algorithm utilized multi-spectral information extracted from 7 Manitoba source waters, and from samples treated with strong base ion-exchange (IX). AMW components between 2.2-4 k Da were strongly associated with the formation of THMs, and more strongly with chlorinated byproducts, determined using Spearman and Pearson coefficients. associations were not improved upon removal of the raw samples from the dataset, indicating that the applied methodology is not specific to IX treatment. Strong associations were also found between initial wavelengths of 226–239 nm and final wavelengths of 257–273 nm, which suggests that absorbing moieties in these ranges are prime precursors in the reaction mechanism to form THMs. A closer look noted that chlorinated THMs were more strongly associated than THMs in general; with brominated byproducts following closely to profiles of UV_{254} - indicating these parameters are closely related.

1. Introduction

Natural organic matter (NOM) plays an important role in the general ecological makeup of ecological and engineered systems.

* Corresponding author.
E-mail address: brezinkk@myumanitoba.ca (K. Brezinski).

https://doi.org/10.1016/j.chemosphere.2019.02.176
0045-6535/

Abbreviations

AMW	Apparent Molecular Weight
DBPs	Disinfection Byproducts
DOW	Dowex
GL	Glenella
HAA	Haloacetic Acids
HPLC	High Performance Liquid Chromatography
HPSEC	High Performance Size Exclusion Chromatography
IX	Ion Exchange
LOD	Limit of Detection
LET	Lettelier
LMW	Low Molecular Weight
MOR	Morris
NOM	Natural Organic Matter
PC	Pine Creek First Nation
PSS	Polysulfonated Salts
RR	Rainy River
SAN	Sanford
SBA	Strong Base Anionic
SEC	Size Exclusion Chromatography
SRNOM	Suwannee Rover Natural Organic Matter
$SUVA_{254}$	Specific Ultraviolet Absorbance at 254 nm
THMs	Trihalomethanes
TTHMs	Total Trihalomethanes
TOC	Total Organic Carbon
UV_{254}	Ultraviolet Absorbance at 254 nm
UVA	Ultraviolet Absorbance

NOM is a ubiquitous class of complex aquatic organic molecules that are ultimately sourced from the breakdown of plant residues, lignin, cellulose and other complex macromolecules from allochthonous (terrestrial) and autochthonous (marine) sources (Eszwald, 2010; Thurman, 1985). As a result of its ambiguous composition, NOM does not have a set defined size distribution, functional group composition, acid-base functionality, or chelating potential. This makes it extremely difficult to model the behaviour of NOM in regards to its impact in potable water distribution systems. This is especially the case when investigating NOM interactions to form disinfection-by products (DBPs), which are known, and heavily monitored, carcinogenic byproducts. Some dominant species of concern include trihalomethanes (THMs) and haloacetic acids (HAAs) - both of which are formed via a complex reaction pathway (Lavonen et al., 2013; Zhai and Zhang, 2011). The work of Zhai and Zhang (2011) provided a greater explanation to the "black box" formation of DBPs by suggesting an intermediate step from high molecular weight (HMW) products to the finalized forms of THMs and HAAs that are closely monitored in water supplies today. Investigators have utilized fractionation methods based on hydrophilicity and molecular weight distributions to formulate a relation between these and DBP formation (Lin et al., 2014); however, these relations have only been shown to be relational and do not include sufficient resolution to definitively predict the formation of these byproducts.

One of the key interests in the study of NOM behaviour is in the establishment of operational parameters through the use of various analytical tools and surrogate parameters. Ultraviolet absorbance (UVA) at various wavelengths have been used to predict properties of NOM such as aromaticity (UVA_{254}) (Her et al., 2008; Cory and McKnight, 2005; Liang and Singer, 2003; Weishaar et al., 2003; Karanfil et al., 2002; Chin et al., 1994; 1997), nitrate concentration (UVA_{210}) (Whitehead and Cole, 2006) and trihalomethane formation potential (UVA_{272}) (Korshin et al., 2009). As of recently, high performance size exclusion chromatography (HSPEC) has found multiple applications in investigating the nature and composition of NOM in a potable water setting. This advantage stems from the multi-spectral nature of chromophoric organic matter which can be subsequently measured by the photodiode array of the HPSEC system; which is simply unattainable when considering only one absorbance wavelength at a time. This is done simultaneously while performing size-separation, thereby providing a multi-spectral, apparent molecular weight (AMW) distribution of the sample. It is suggested that wider application of HPSEC as a NOM monitoring tool can provide sufficient resolution to expand our current understand of NOM characterization. The work of Yan et al., 2012 used the slope of absorbances between select wavelengths as a means to ascertain the relation between AMW and wavelength. Additionally, a bevy of uses of HPSEC, in addition to other NOM characterization methods, have been employed to help researchers understand the reactivity and fate of NOM in the study of drinking water (Pan et al., 2016).

The use of measuring and monitoring AMW of NOM fractions (Ruhl and Jekel, 2012) has shown interesting applications in analysing processes involving physical removal such as Membr. filtration (Chabalina et al., 2013; Lee et al., 2004; Kim et al., 2002; Zhou et al., 2000). AMW ranges have also been tied to reactive forms of NOM, such as humic substances, which relate to select AMW ranges in the HPSEC chromatogram (Phetrak et al., 2016; Lewis et al., 2012). Alternatively, the work carried out by Drikas et al. (2011) examined NOM removal as it relates to the removal of size distributions calculated as weight average molecular weight Mw, following ion-exchange (IX). Certain conventional treatments, such as coagulation, have shown selective removal of high AMW NOM; while IX has shown a more equal distributive removal of NOM (Drikas et al., 2011; Mergen et al., 2009). The increased prevalence of strong base IX application for NOM removal had led to increased interest in the mechanisms and the components removed in the process.

This work hopes to explore the characterized removal of NOM components following strong-base IX application for synthetic and 7 waters sourced from Manitoba, Canada. This will be done through a multi-wavelength, size-dimensional analysis using HPSEC, coupled with an iterative approach which can further parse the contributions of various UV absorbing moieties to THM formation. It is speculated that chlorinated versus brominated byproducts include different NOM precursors that are not viably resolved with conventional surrogate parameters and characterization techniques. With the aid of numerical techniques and correlation parameters, relationships between surrogate measurements for NOM - such as UV_{254}, total organic carbon (TOC), and specific ultraviolet absorbance at 254 nm ($SUVA_{254}$) - will be used to trace relationships to regions of interests in the HPSEC chromatogram.

2. Materials and methods

2.1. Synthetic and source waters

Synthetic water was prepared using the Suwannee River NOM (SRNOM) (International Humic Substances Society, St. Paul MN) standard prepared at concentrations of 100 mg L^{-1} in deionized water. Source waters were obtained from the raw water intake from seven (7) locations in Manitoba, Canada. The locations include: Sanford (SAN), Glenella (GL), Pine Creek First Nations (PC), Duck

Bay (DB), Morris (MOR), Letellier (LET), and Red River (RR). Samples were stored at 4 °C in a dark cold room for no more than a week of time. It was confirmed upon initial sampling and after 1 week of cold-storage that there was no drift in the recorded concentration of TOC.

2.2. Ion exchange sorption

A series of strong-base anionic exchange resins were initially preconditioned and rinsed with 1 M NaCl and deionized water solutions, respectively. Samples were volumetrically dosed using wet doses converted from dry doses according to specifications of the resin manufacturer. Samples were dosed at 3 and 5 mg L^{-1} according to work performed by others (Flowers and Singer, 2013; Comstock et al., 2011; Apell and Boyer, 2010) and mixing time carried out by Najim and Trussel (2001). Samples were contacted in 4 oz. amber glass bottles and allowed to come to equilibrium using an orbital shaker (Labnics Equipment, Fremont CA) at 100 rpm. The four strong-base anionic (SBA) resins all performed similarly, and the results are summarized as supplemental information (Fig. S.3). All HPSEC analyses were carried out using the DOWEX (DOW) TAN-1 resin.

2.3. HPSEC analysis

HPSEC was performed using a Waters e2696 HPLC module (Waters Associates, Milford, MA) with a temperature control module and column heater, coupled with a Waters 2998 photo-diode array detector capable of operating within the 190–400 nm range. Sample injections were set at 10 μL and an isocratic flow of 1.0 mL min^{-1} was set for the eluent rate. System components and data acquisition was controlled using Empower3 software (Waters associates, Milford MA). The analysis involved a BioSep-SEC-S2000 silica column, 300 × 7.8 mm (Phenomenex, Torrance CA). Mobile phase included a 100 mM phosphate buffer (0.0016 M Na_2HPO_4 and 0.0024 M NaH_2PO_4 to yield a pH of 6.8). 75 mM KCl was added to yield a final ionic strength of 0.1. With an ionic strength of 0.1 polystyrene sulphonate (PSS) standards have been shown to have similar coiled shapes as humic substances (Zhou et al., 2000). An increased ionic strength of 0.1 has been shown to minimize Fuoss theory effects; where in the presence of salts, cations are attracted to the carboxylate anions of organic acids and causes them to coil. In low salt solutions Macromol. tend to stretch, which leads to an increased intramolecular coulombic interaction in the macromolecule chain (Jan and Breedveld, 2008). This has the effect of increasing hydrated radii, therefore altering their shape (Ha and Thirumalai, 1992; Fuoss and Strauss, 1948). All samples were pre-filtered with a 0.45 μm polyvinylidene fluoride syringe filter (Merck Millipore, Billerica MA) and adjusted to a similar pH and ionic strength conditions as the carrier solvent using 50% NaOH and Na_2HPO_4, respectively. This was done following overnight degasification to prevent bubble formation during HPLC separation.

Various molecular weight calibrants for the size exclusion analysis of humic substances have been employed by researchers. The most common ones include polysulfonated salts (PSS) (Liu et al., 2010; Korshin et al., 2009; Chow et al., 2008; Perminova et al., 1998; Chin et al., 1994) and polyethylene glycol (PEG) (Her et al., 2008; Zhang et al., 2008). In this work, PSS standards of 1.7 K, 5.2 K. 7.5 K, and 16 K (Scientific Poly. Products Inc., Ontario NY) were used and prepared at concentrations of 1 g L^{-1}. The 1.7 K PSS standard displayed peak splitting, therefore a 200 apparent molecular weight (AMW) PEG (Alfa Aesar, Haverhill MS) standard was used as a replacement for the low molecular weight standard (Fig. S.1). The calibration curve with the inclusion of the 200 Da polyethylene glycol standard yielded an R^2 of 0.9999 (Fig. S.1). HPSEC work was performed within the day of calibration as the column conditions and instrument drift can alter the regression. Standards were detected at 230 nm corresponding to their maximum peak absorbance tested at three wavelengths (Fig. S.2); while samples were detected at various wavelengths in the range of 200–400 nm simultaneously.

2.4. Peak intervals

All computation and numerical methods were carried out in the Matlab R2016a (MathWorks Inc., Massachusetts) environment. HPSEC values were imported into the Matlab workspace as a structured array and sequenced for signal analysis. Each peak was detrended from the baseline in order to remove the contribution due to instrumental noise, and to distinguish statistically significant peaks from noise and impurities. This was done by computing the limit of detection (LOD) for the absorbance values, calculated as $x_{blk} + 1.96 s_{blk}$ - where x_{blk} is the mean of the noise and s_{blk} is the standard deviation of the noise.

The peaks were sequentially integrated over wavelength ranges between 220 and 400 nm. The wavelength ranges chosen include: 220–240 nm (R2040), 240–272 nm (R4072), 272–365 nm (R7265), and 220–365 (RTot). These ranges were selectively chosen as other investigations using absorbance – such as the application of spectral slope parameters (Helms et al., 2008) – showed correlations with these ranges and other water characteristics. Additional intervals were selected based on AMW, and were identified based on significant absorbing peak moieties identified in Fig. 1 for the 7 water sources tested. Ranges selected include: 0.6–1.1 k Da (Peak A), 1.6–2.1 k (Peak B), and 2.2–4.0 k Da (Peak C).

A script was developed to sequentially scan and evaluate the integral over different wavelength ranges of the SEC profile. This was done by setting the initial index λ_i, $i \in \{1, 2, \ldots N-1\}$ and final index λ_j, $j \in \{i+1, i+2, \ldots N\}$ within a narrow range at a low wavelength, evaluating the integral, then incrementing j by 1. Once the surface is scanned in its entirety, the index for i is incremented

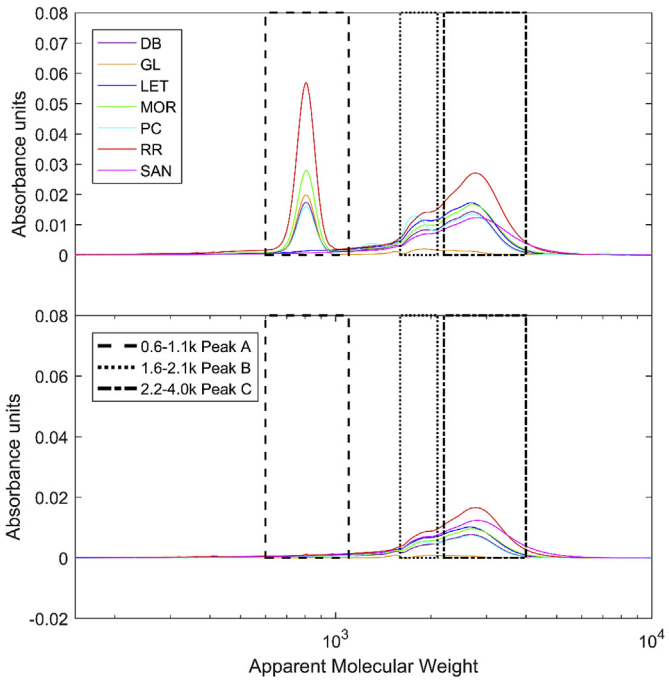

Fig. 1. Identified AMW peaks identified as significant contributors to chromophoric organic matter; with peaks of interest identified at (top) 254 nm and (bottom) 280 nm.

by 1 and the process continues until completion. This produces an array of evaluated integrands that represents each slice of the chromatogram - as well as every iteration of ranges in wavelength between 220 and 400 nm.

2.5. Apparent molecular weight determination

AMW and polydispersity indices were used to determine the molecular weight distribution determined using information retrieved from HPSEC peak responses at UV_{254} (Zhou et al., 2000). Number averaged molecular weight (M_w), weight averaged molecule weight (M_n), and polydispersity (ρ) were determined from the following equations adopted from Yau et al. (1979), and used by others (Huang et al., 2016; Cabaniss et al., 2000; Zhou et al., 2000; Chin et al., 1994):

$$M_w = \frac{\sum_i h_i}{\sum_i \frac{h_i}{M_i}} \quad (1)$$

$$M_n = \frac{\sum_i h_i M_i}{\sum_i h_i} \quad (2)$$

$$\rho = \frac{M_w}{M_n} \quad (3)$$

where h_i corresponds to the baseline height in the chromatogram at retention time *i*. h_i is a function of the MW_i of a compound and it's frequency f_i as described by Zhou et al. (2000). M_i corresponds to the equivalent calculated molecular weight of a compound at retention time *i*. Values for ρ indicate whether or not a heterogenous sample such as NOM has a high or low MW dispersivity. A value of 1 indicates a uniform sample, while a number that deviates from 1 indicates dispersivity (Kottisch et al., 2016).

2.6. Correlation coefficient

In order to test the correlation between HPSEC peak characteristics and other water quality parameters, a series of statistic tools were utilized. The Pearson correlation coefficient was one of such tools used to provide a relation between variable x and y given they are either on an interval or a ratio scale. Equation (3) provides the mathematical formulation for the Pearson correlation coefficient.

$$r = \frac{\sum_{i=1}^{N}(x_i - \bar{x})(y_i - \bar{y})}{\sqrt{\sum_{i=1}^{N}(x_i - \bar{x})^2 \sum_{i=1}^{N}(y_i - \bar{y})^2}} \quad (4)$$

where $\bar{x}$ and $\bar{y}$ are the mean values for variable *x* and *y*, respectively; x_i and y_i and the values for variables *x* and *y* at sample number *i* respectively; and *N* is the total number of samples. Pearson coefficient values can range from 1 to −1, where 1 is a perfect positive correlation, −1 is a perfect negative correlation, and 0 is no correlation. An additional parameter was calculated known as the Spearman coefficient, summarized by Equation (4).

$$\rho = \frac{3\sum d_i^2}{n(n^2 - 1)} \quad (5)$$

where *n* is the number of samples points; and d_i^2 is the difference between variables squared. The Spearman coefficient takes into account the effect of one monotonic variable which either increases or decreases as another variable increases. *p* values were determined in order to test no correlation versus the alternative null hypothesis.

2.7. Laboratory analysis

Total THMs (TTHMs) where determined according to Standard Methods 5710B (Rice et al., 2012). THM analysis was recorded as the measurement of THM4 which comprises of the species, chloroform ($CHCl_3$), bromoform ($CHBr_3$), chlorodibromomethane ($CHClBr_2$) and bromodichloromethane ($CHCl_2Br$). This definition is consistent with those outlined in the Canadian Guidelines for Drinking Water Quality (Health Canada, 2006) and World Health Organization (WHO) (WHO, 2017). Gas chromatography for THM analysis was carried out using an Agilent 7820A system (Agilent, CA) equipped with electron capture detection and a CombiPal CTC Analytics autosampler (CTC Analytics, Zwingen). Separation was performed with an Agilent DB-5 column, with dimensions: 30 m × 0.32 mm x 0.24 μm. Detection limits for THM4 analysis were determined to be 10 μg L^{-1}. TOC analysis was performed using a FormacsHT Series High-Temperature TOC Analyzer (Skalar Inc., Georgia) coupled with FormacsHT/TN Total Carbon (TC)/Total inorganic carbon (TIC) detection (ND25). DL was determined to be 0.4 mg L^{-1} pH measurements were performed using a Fisher Scientific Accument 50 pH meter (Fisher Scientific, NJ). UVA_{254} was carried out using an Ultrospec 2100 UV/Vis spectrophotometer (Biochrom, Cambridge) with a quartz cuvette. Specific Ultraviolet Absorbance at 254 nm ($SUVA_{254}$) was determined according to USEPA Method 415.3 (Potter and Wimsatt, 2005).

3. Results and discussion

3.1. Molecular weight evaluation

The effect of SBA treatment on the molecular weight distribution of the source water was evaluated. A script was developed to compute the weight-averaged and number-averaged molecular weights of the samples according to Equations (1)–(3). A summary of the results is displayed in Table 2. Findings display a general trend of increasing M_n and M_w with increasing resin dose from 3 to 5 mg L^{-1}. This highlights the ability for IX to target the low molecular weight (LMW) range of the AMW distribution, consistent

Table 1
Properties of ion-exchange resins.

Resin	Structure	Capacity (meq mL^{-1})	Water Content % (m/m)
DOW TAN-1	Polystyrene, Quaternary Amine	0.7[a]	70-82 (65–77)
Purolite A502P	Polybenzene, Quaternary Amine	0.85[a]	66-72 (63–69)
Amberlite PWA9	Polyacrylic, Quaternary Amine	0.8[b]	66-72 (61–68)
Purolite A860	Polyacrylic, Quaternary Amine	0.8 [a]	52-72 (52–69)

[a] Chloride-form.
[b] Hydroxide-form.

Table 2
Weight-averaged, number-averaged and polydispersity index for 7 water sources contacted with 3 and 5 mg L^{-1} doses of DOW TAN-1 resin.

		M_w	M_n	ρ
DB	Raw	3726	3735	0.9976
	3 mg L^{-1}	4634	4706	0.9963
	5 mg L^{-1}	5521	5778	0.9565
GL	Raw	3985	4347	0.9676
	3 mg L^{-1}	4523	4696	0.9644
	5 mg L^{-1}	4736	5078	0.9335
LET	Raw	3763	3775	0.9969
	3 mg L^{-1}	4817	5016	0.9622
MOR	Raw	3785	3799	0.9962
	3 mg L^{-1}	4648	4692	0.9898
	5 mg L^{-1}	4680	4784	1.0017
PC	Raw	3760	4097	0.9569
	3 mg L^{-1}	4096	4131	0.9915
	5 mg L^{-1}	4109	4553	0.9621
RR	Raw	5400	5591	0.9632
	3 mg L^{-1}	4663	4977	0.9419
	5 mg L^{-1}	3706	3721	0.9964
SAN	Raw	3837	3857	0.9947
	3 mg L^{-1}	4014	4064	0.9876

with the findings of Kaewsuk and Seo (2011) who noted a selective removal of LMW aromatics and humics following IX. Additionally, the findings show a shift in ρ towards a lower value following IX, indicating an increase in the value of M_n in the equation for $\rho = M_w/M_n$. A notable exception to this trend is seen for RR 5 mg L^{-1} and MOR 5 mg L^{-1}, indicating a misattributed peak identified during peak selection. The only other exception is PC which had ρ increased following both doses. PC had the lowest starting value for ρ amongst the dataset, which may lead one to conclude that IX has a normalizing effect on the AMW distribution. This would be the case when steric effects are involved and large moieties are removed due to outer sphere complexation while smaller moieties readily enter the inner porous structure of the macroporous resin. As a result, IX has the ability to remove a wide distribution of AMW as compared to treatments such as coagulation (Lewis et al., 2012; Chow et al., 2008). Samples for LET and SAN were only contacted with doses of 3 mg L^{-1} as at doses of 5 mg L^{-1} the remaining peaks were not baseline separated and quantifiable.

3.2. 3D-HPSEC contour plots

HPSEC chromatograms are used to better appreciate the multi-wavelength, AMW distribution of the samples measured. HPSEC profiles also provide researchers with a competitive advantage in NOM profiling that is simply unattainable using parameters such as UVA_{254}, TOC, and $SUVA_{254}$. Fig. 2 displays the resulting chromatograms following SBA resin treatment. The figure helps to illustrate the component ranges specifically targeted by two different doses of SBA resin.

Common features can be seen between samples from DB, MOR, and LET which all show large removals of moieties between the AMW range of 2.4 k − 3.1 k Da. The bulk removal of these components, as well as those at LMW, would explain the shift in M_n and M_w towards higher values indicated in Table 2. These large bulk peaks would be identified as those labeled as Peak C, representing AMW in the range of 2.2-4 k, noted in Table 1. Additionally, components attributed as Peak C would compromise the bulk of NOM - including fulvic acids and humic acids - as they mirror the SRNOM standard found within a similar range (Fig. S.3). All samples, with the exception of LET, saw a reduction in a small narrow peak identified as Peak A (0.6–1.1 k Da) in Fig. 1, which may be associated with LMW acids or building blocks (Brezinski and Gorczyca, 2019; Hidayah et al., 2016; Huber et al., 2011). This association was also made by Liu et al. (2010) who investigated a similar removal trend in the Peaks A's AMW range following TiO_2 photocatalytic treatment. GL is seen as a noticeable exception as the water source was found to have a peak C that was far lower than the other source waters (Fig. 1), therefore the effective removal of the peak (as a % of max peak) would not be apparent to begin with. The bottom subplot of GL (5 mg L^{-1}) is also distinctly different from the top subplot as Peak B and C were so close to baseline that they appear as similar contours. Additionally, the water table for GL summarized in Table S.1 and S.2 lists GL as having the lowest starting TOC, UVA_{254}, and THM4 amongst the source waters; which can lead one to suppose there may be a connection between the size of Peak C and these parameters. Other peaks of interest include the pronounced removal of Peak B (1.6k-2.1 k Da) found in the resulting chromatogram for the PC treated sample. SAN water source was excluded from the contour analysis as peak chromatograms were not adequately reproducible and baseline separated.

3.3. Molecular weight and wavelength intervals

3.3.1. Basic water quality trends

Correlations between variables can be found given an adequate dataset is available and a trend exists between the variables selected. The Pearson and Spearman correlation coefficients were described in Section 2.6 and were applied to the dataset as a whole, as well as a separate dataset excluding raw samples. Excluding raw samples allows for the determination as to whether or not the associations are treatment specific; as improvements with the addition of the raw samples will only strengthens the case that the associations are universal. Figs. 3 and 4 (Table S.4 and S.5) provides a summary of coefficient values between water parameters/THM4 values and peak associations for Spearman and Pearson coefficients, respectively. As a rule of thumb, coefficients exceeding ±0.5 and approaching a perfect correlation of ±1 are considered to have a large strength of association. Correlations with coefficients between ±0.1 - ±0.3 and ± 0.3 - ±0.5 are considered to have small and medium strengths of association, respectively.

Among the AMW and wavelength peaks profiled, the strongest Pearson correlation coefficient for the basic water quality parameters was found to exist between the prevalence of Peak B and TTHM formation with a coefficient of 0.76 ($p = 0.00$). A strong correlation was also found to exist between Peak B and TOC (0.55, $p = 0.01$), more so that Peak C and TOC (0.12, $p = 0.60$); leading one to conclude that components within the range of Peak B (1.6–2.1 k Da) have a higher organic carbon character than components of Peak C (2.2-4 k Da). This may be the case as Peak B was the only range that exhibited a medium/strong correlation with TOC. In the previous section, Peak C was found to be heavily targeted by IX treatment; however, it does not describe what the nature of that removal is on the bulk of NOM. It may be the case that Peak B may have properties that are more consistent with those attributed to fulvic acids (FA), while Peak C - with a higher molar absorptivity coefficient and higher M_n and M_w (Chin et al., 1994) - would have properties consistent with those attributed to humic acids (HA). Medium associations were found between TTHM and Peak A (0.53, $p = 0.01$), R2040 (0.52, $p = 0.02$), and RTot (0.53, $p = 0.01$); with the latter two cases showing better association due to the inclusion of Peak A which is only present at low wavelengths (See Fig. 1). All other correlations either had low association - as is the case with TOC - or very poor correlation, such as with SUVA and $CHBr_3$. Since $SUVA_{254}$ calculation includes the inverse of TOC, it is to be expected that $SUVA_{254}$ would have a corresponding association in the negative direction (i.e. the inverse of a positive correlation is a negative correlation) but still poor correlation overall. $SUVA_{254}$ is a

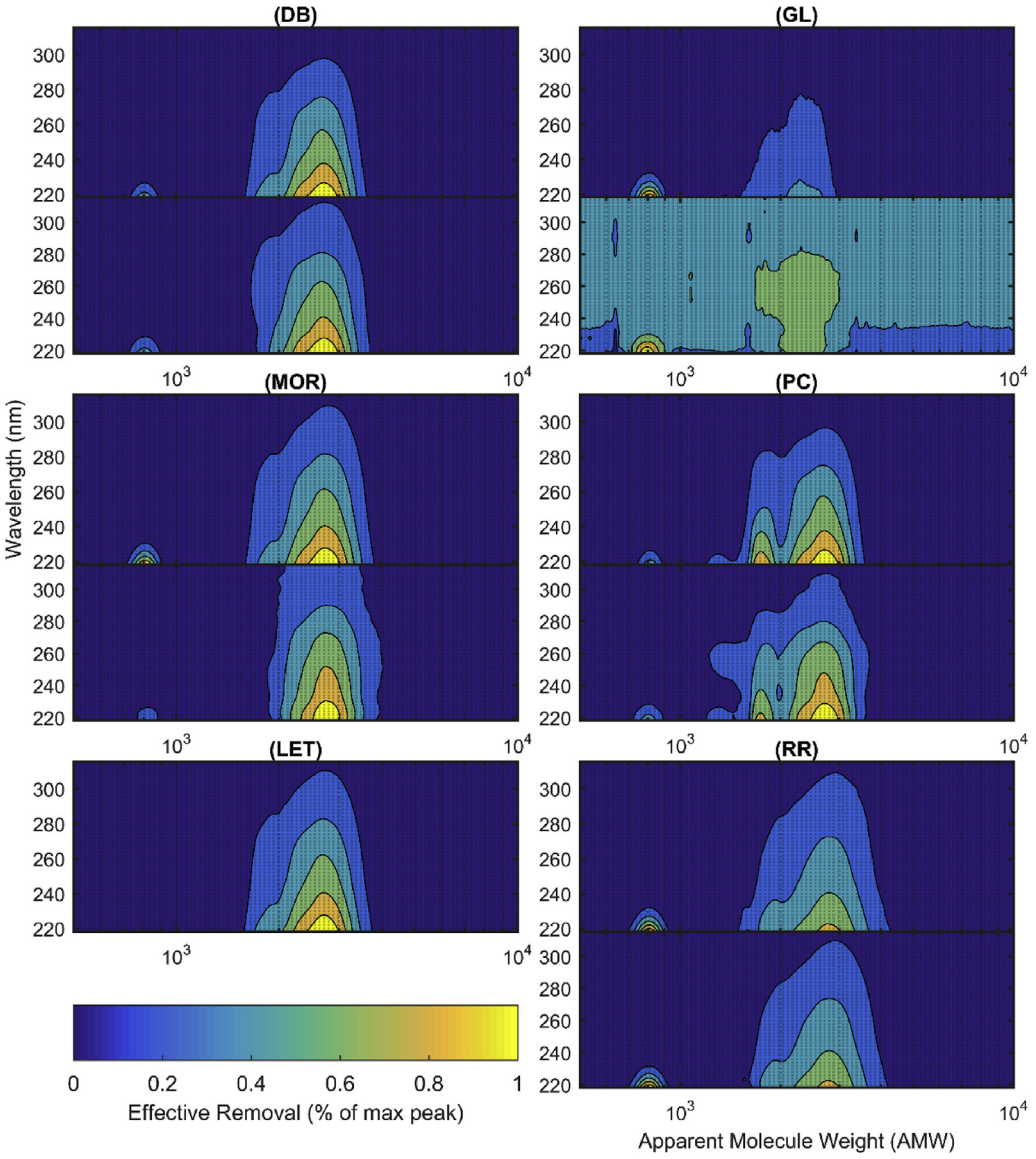

Fig. 2. Effective removal for water sources treated with DOW TAN doses of 3 mg L^{-1} (top subplot) and 5 mg L^{-1} (bottom subplot). Effective removal was determined from the subtraction of raw peak absorbance by the associated treated water absorbance. Colorbar is based on % of max peak for simplification.

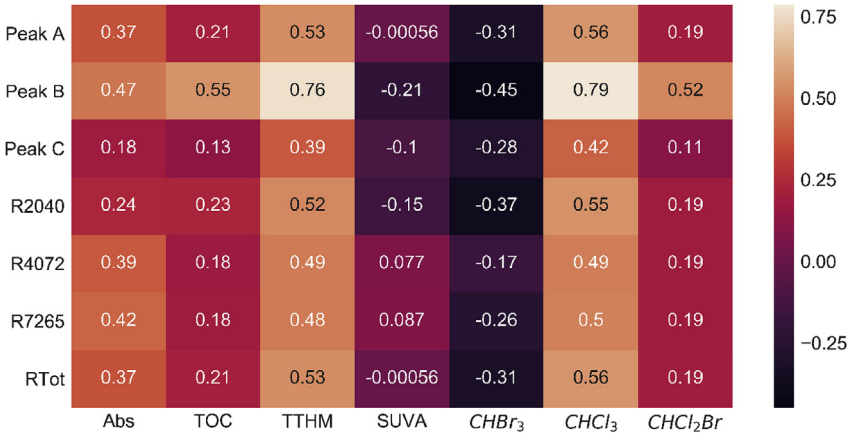

Fig. 3. Pearson correlation parameters for a series of integrated peak trends with common water quality and THM species measurements (n = 19).

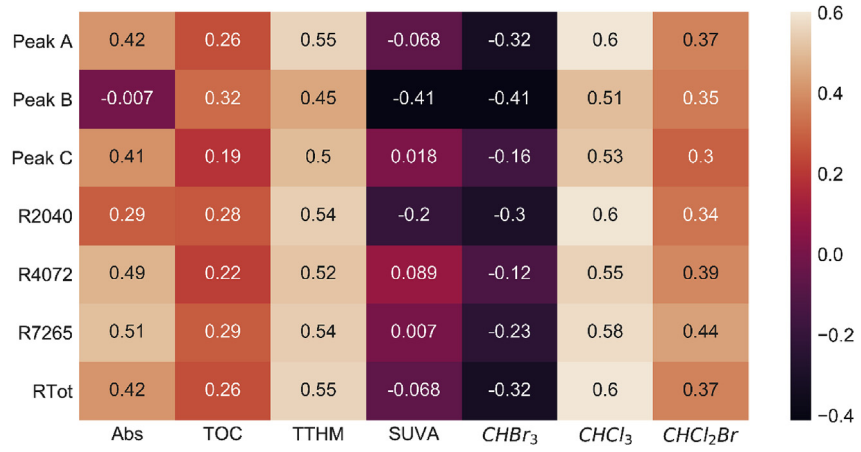

Fig. 4. Spearman correlation parameters for a series of integrated peak trends with common water quality parameters and THM species measurements (n = 19).

surrogate measurement for aromatics per unit carbon, and while TOC and Abs may be related to peak area to an extent, it does not necessarily mean a relationship exists with a measure of $SUVA_{254}$.

The Spearman correlations shown in Fig. 4 did not improve the association between parameters. Most correlations with TOC values improved to a small degree, while some associations worsened, such as with Peak B and TTHM. Improvements were made for ranges that were not Peak B, such as for $CHCl_3$, $CHCl_2Br$, TTHM, TOC and Abs. Since the Spearman coefficients accounts for non-linear associations, the improved values for TOC could be indicative of a potential monotonic relation between absorbing moieties and carbon content. The one exception would be the strong association mentioned prior between Peak B and TOC (0.55, $p = 0.01$), which worsened to 0.45 ($p = 0.18$) when evaluated using the Spearman coefficient. Since Peak B was the only one effected, it strengthens the case that Peak B and TOC are highly correlated with one another linearly. Additionally, adjusted correlation coefficients (adj. R^2) were determined for every iteration of interval and water parameter, with values listed in Table S.3 for reference. For TTHM the only interval which exhibited a somewhat strong adj. R^2 was Peak B at 0.58. A strong adj. R^2 was also found for Peak B and TOC (0.3), and a weaker relation was determined between TTHM and all 4 wavelength intervals: 0.27, 0.23, 0.23, and 0.28 for R2040, R4072, R7265, and RTot, respectively. These values echo the values of the Spearman coefficient, as they are both tests for linearity in sample sets. The Spearman coefficient, however, is also predicated on the normalized distribution of the sample set. Table S.3 lists the Pearson correlation of skewness for each AMW and wavelength interval. Many sample sets have poor distributions (i.e. 0 is perfectly normalized) as they were retrieved from many sources, both raw and treated, and the samples set was limited to 19.

3.3.2. Trihalomethanes

Similar to the previous section, Pearson and Spearman correlation parameters were recorded for the THM4 species, with the exception of Dibromochloromethane ($CHClBr_2$). Dibromochloromethane was recorded to have concentrations that were either below the instrumental detection limit or had levels of variance that exceeded the recorded mean values (see Table S.2). It follows that with the strong relation between TTHM peaks and certain peak intervals, select THM4 species may be correlated as well. A summary of the correlation parameters is displayed in Fig. 4.

When considering chloroform ($CHCl_3$) alone, we see all Pearson and Spearman coefficients improve from their TTHM values listed in Fig. 3. Consequently, a strong correlation between Peak B and TTHM 0.76 ($p = 0.00$) is due to the fact that $CHCl_3$ is inclusive in the measurement for TTHM. The strongest association is found between Peak B and $CHCl_3$ (0.79, $p = 0.00$, adj. $R^2 = 0.59$), with very strong coefficients ranging from 0.51 to 0.6 for the other intervals. Another strong correlation is found between $CHCl_2Br$ and Peak B (0.52, $p = 0.02$), which is not found with any other sample interval, and disappears when evaluating the Spearman coefficient. This may show a clear linearized trend; however, it is not supported by the associated adj. R^2 of 0.22 (Table S.3).

The coefficients for $CHBr_3$ tells us a different story, that is there is an inverse relationship between peak sizes and the formation of $CHBr_3$. A possible explanation for this is can be found in the work of Boyer and Singer (2005) and Phetrak et al. (2016). In the work of Phetrak et al. (2016), the authors noted that when NOM fractions are removed by SBA resin, bromide is removed as well. Since high/low peak areas follow from high/low concentrations of $CHCl_3$ (>0.51) and high/low TTHMs (>0.45) but low/high concentrations of $CHBr_3$, it stands to reason that bromide is more incorporated in total TTHMs produced. Hong et al. (2017) noted this was the case at higher chlorine doses, therefore this relationship may be due to the chloride and bromide balance in solution following SBA resin application. It was noted in the work of Pan and Zhang (2013), that greater presence of bromide in solution shifts TTHM formation towards brominated-THM species that act as important intermediaries towards the formation of the finalized THM products. SBA resin has different selectivity for NOM, bromide and chloride; therefore, increasing resin dose may remove more bromide than NOM and chloride, thereby showing an inverse relationship in $CHBr_3$ formation. Since bromide and chloride concentrations were not accounted for, the reasoning remains speculative. Boyer and Singer (2005) provides a similar suggestion, as bromide concentration in the waters tested were impacted by the water alkalinity - more so that chlorine and iodine in THM formation (Kaewsuk and Seo, 2011). Another explanation was suggested in the work of Rodrigues et al. (2007) who noted FA concentration was inversely proportional to brominate THM species, therefore with a greater proportion of FA remaining, the recorded $CHBr_3$ will not follow suite. This is further in line with the conclusions made earlier where Peak B and Peak C were more characteristic of FA and HA, respectively. Peak C was noted to be more greatly impacted by SBA treatment, leaving Peak B (FA) as a greater proportion of NOM remaining; and consequently, inversely correlated to $CHBr_3$ formation. Formation for $CHCl_3$ also improved using the Spearman coefficient, especially among correlation coefficients for R2040, R4072, R7265 and RTot: 0.6 ($p = 0.00$), 0.55 ($p = 0.01$), 0.58

($p = 0.01$), and 0.6 ($p = 0.00$), respectively. Values for $CHCl_2Br$ provide a middle ground between the formation of $CHCl_3$ and $CHBr_3$, as the correlation coefficients seem to be related to the halogen used in the formation of the specific THM species.

With the removal of NOM samples, select parameters were improved from their values (Table S.4 and S.5). Certain associations were seen to improve in the removal of the raw samples. This was found to be the case in the improvements for Spearmans for R2040 and TTHM (0.53–0.63), Pearsons for R2040 and $CHCl_3$ (0.54–0.63), and Spearmans for R2040 and $CHCl_3$ (0.59–0.67). Since these improvements were all associated within the range R2040, it comes to reason that IX may be specifically targeting components at this early wavelength range, or regions with high changes in molar absorptivity. As the sole exceptions, it suggests that they act as better markers for treatment with SBA resin, as opposed to being better overall indicators in the methodology. One explanation may be due to the ability for SBA resins to preferentially remove hydrophilic (HPI) components (Phetrak et al., 2016; Mergen et al., 2008); thereby allowing the remaining hydrophobic (HPO) components to be the sole contributors to $CHCl_3$/TTHM formation. Therefore, one can suppose that the HPO moieties that make up the bulk of the remaining NOM are highly reactive and would have high levels of specific $CHCl_3$ formation (i.e. conc. $CHCl_3$ per mg carbon) (Brezinski and Gorczyca, 2019; Hu et al., 2015; Gough et al., 2012). This effect is not mirrored by any other AMW or wavelength interval. The lack of improvement upon removal of the Raw samples helps to illustrate that samples treated with SBA resin do not have trends in their chromatograms that are specific to the treatment used. Therefore, the methodology used does not bias datasets based on treatment, at least for treatment with SBA resin. This further supports the novelty of this work, as it is more encompassing to many source waters, and potentially, to more treatment methods.

3.4. 3D-HPSEC basic water quality interval array

In Section 2.4, an array of values was extracted from each unique spectrum and are summarized in Figs. 5 and 6 corresponding to Pearson and Spearman coefficients, respectively (tabulated in Table S.4 and S.5). Strong associations can be seen with UVA_{254} (labeled as Abs), with high levels approaching −0.42 and TTHM levels approaching −0.52. Consistent with the findings in Section 3.2, TTHM is heavily influenced by UVA moieties at earlier wavelengths, i.e. R2040; however, it is important to note these plots do not provide information on any trends in AMW distribution – such as the prevalence of Peak A. Trends of Abs and TOC do not shift with increasing initial/final wavelength, indicating these parameters are not affected by groups of UVA moieties in particular. The SUVA plot also has a relatively low degrees of associations, therefore they were excluded from further consideration.

Spearman coefficients provides a more impactful description between these parameters and their trends. The largest associations are again seen for Abs and TTHM, with the largest values exceeding −0.52 and −0.57, respectively. Abs has the largest coefficients at $\lambda_{int} = 226–239$ and $\lambda_{fin} = 257-273$ (further identified as S1 for convenience), with a smaller patch appearing at $\lambda_{int} = 243–256$ and $\lambda_{fin} = 248-265$ (identified as S2). S1 and S2 both appear in regions that are typically associated with aromatic and aromatic-like components, which is consistent with the notion that UV_{254} is measured at 254 nm. S1 is apparent in the plot of TTHM, which again is consistent with the widespread use of UVA_{254} as a

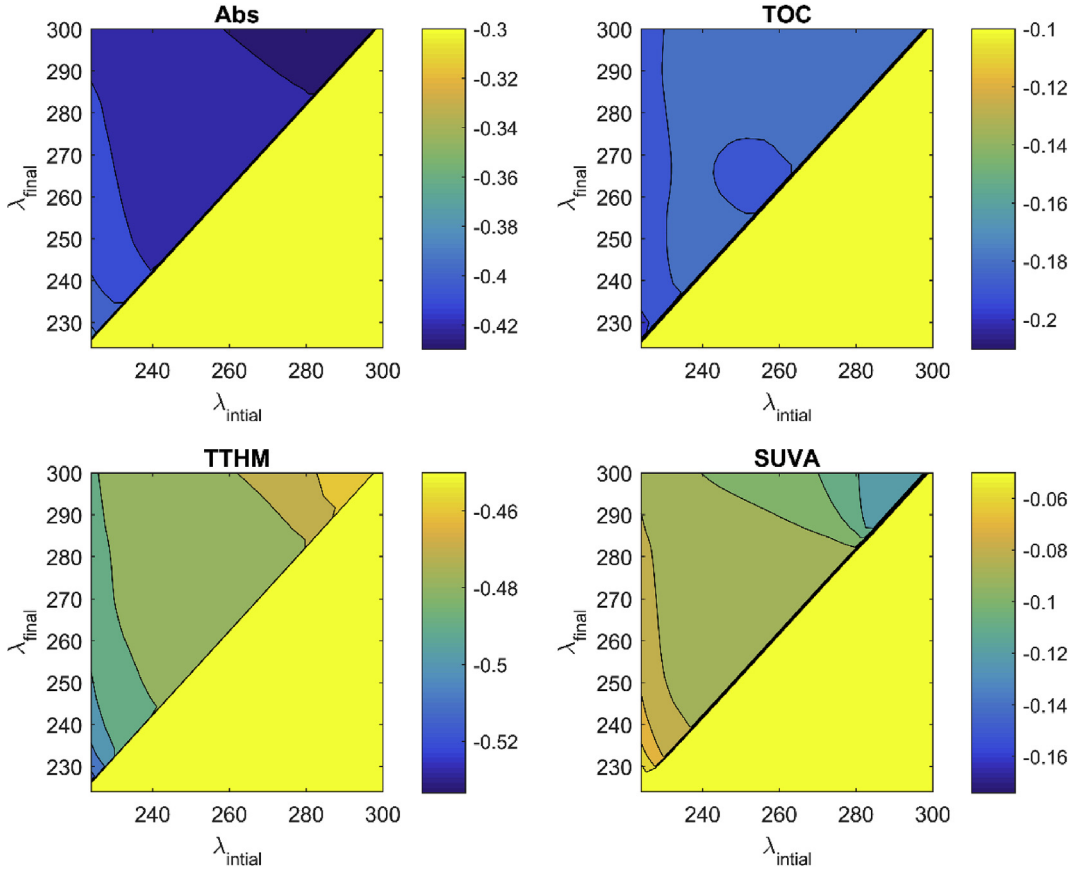

Fig. 5. Pearson correlation coefficient evaluated for the integral array for N = 19 samples.

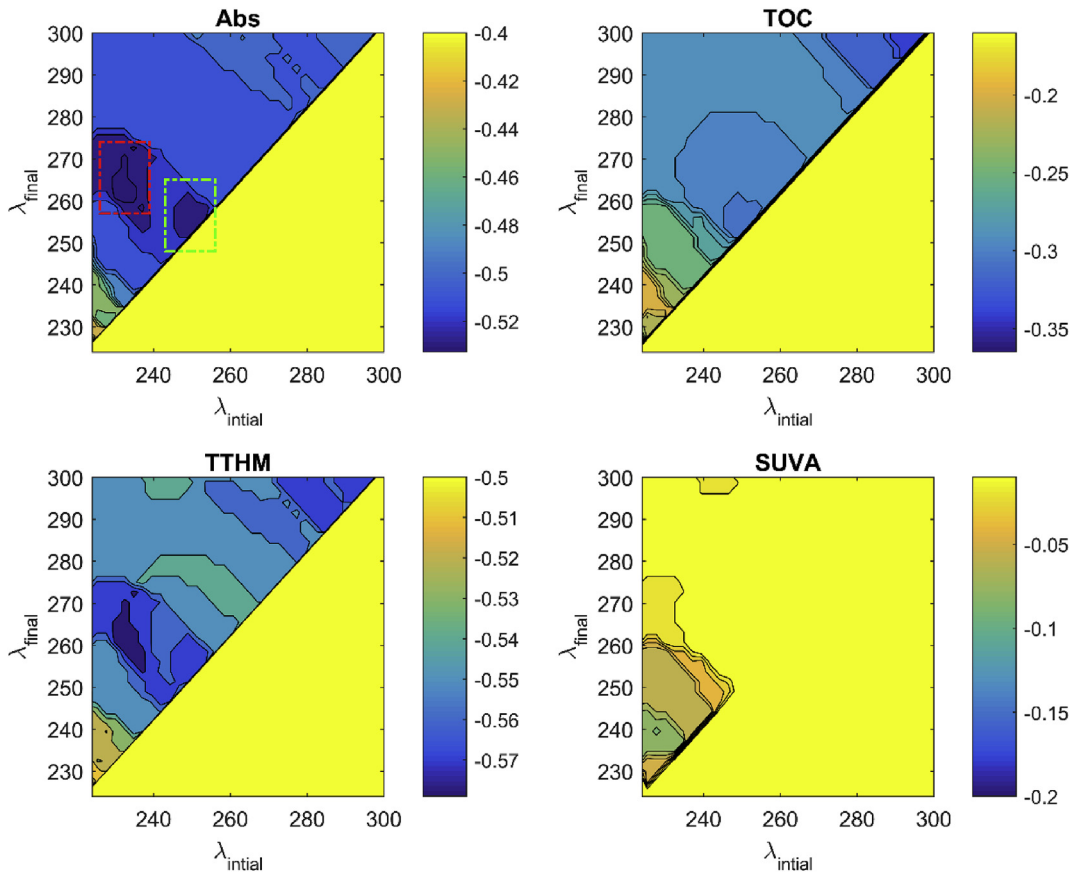

Fig. 6. Pearson correlation coefficient evaluated for the integral array for N = 19 samples. The red dashed box represents absorbance moieties at $\lambda_{int} = 226–239$ and $\lambda_{fin} = 257\text{-}273$ (S1), and the green dashed box for moieties at $\lambda_{int} = 243–256$ and $\lambda_{fin} = 248\text{-}265$ (S2). (For interpretation of the references to colour in this figure legend, the reader is referred to the Web version of this article.)

way of monitoring THM formation. It does however, illustrate the degree to which UVA_{254} only approximates TTHM formation spectroscopically, but lacks the accuracy necessary to predict it quantitatively – as these models only indicate parametric trends. The plot for TOC shows an inverse relationship as a function of increasing wavelength, with the greatest correlation at larger wavelengths. It is important to note that while a trend might be seen using the Spearman coefficient, it does necessarily mean a trend exists as a relationship may very well be linear; but both coefficients are displayed for purposes of comparison. Trends for $SUVA_{254}$ were low to non-existent, as also demonstrated in earlier examinations of $SUVA_{254}$, therefore they were removed from further consideration.

3.5. 3D-HPSEC trihalomethane interval array

In Fig. 7 Pearson and Spearman coefficients are compared side by side for direct comparison. We see similar trends as those observed for TTHM, that is, high correlation at earlier wavelengths for $CHCl_3$ (−0.55); however, the trends for $CHBr_3$ and $CHCl_2Br$ are both low, with coefficients reaching 0.2 and −0.18, respectively. The identified regions of interest for the Spearman coefficient tell a different story. We see consistency in the presence of region S1, identified prior in Fig. 6, in the formation of $CHCl_3$ - with a high coefficient approaching −0.6. We see the same region S1 in the contour for $CHCl_2Br$ (−0.50) but absent from the contour of $CHBr_3$. This region may be consistent with components of NOM that contribute to the formation of chlorinated byproducts, but not brominated byproducts. It was noted in Section 3.3.2 (Fig. 4) that the trends in $CHCl_2Br$ were a middle ground between coefficients found for $CHCl_3$ and $CHBr_3$. Fig. 7 provides a further insight that was not apparent otherwise, that is, the precursor product has a relationship with the halogen used to form the end-product THM. The prevalence of region S2 was identified on $CHCl_2Br$ as well, which may lead one to consider that the measurement for UVA_{254} may aid in predicting the formation of $CHCl_2Br$ more so than any other THM product. This observation follows from work that has found that brominated-THM formation results from aromatic intermediary products in solution that would have high absorbance values at 254 nm (Zhai and Zhang, 2011; Jiang et al., 2017). This is still speculation as the association in this region is low (0.15). A smaller region of interest was identified in the formation of $CHBr_3$, identified as S3; however, the region exhibited a low association of 0.15. Provided a larger sample size was carried out, further trends could then be extracted from the resulting chromatogram and a better appreciation for this method can be carried out.

4. Conclusions

In this work, UVA moieties from several raw water sources were characterized and quantified using numerical and statistical methods. These features were extracted from 3D-chromatograms

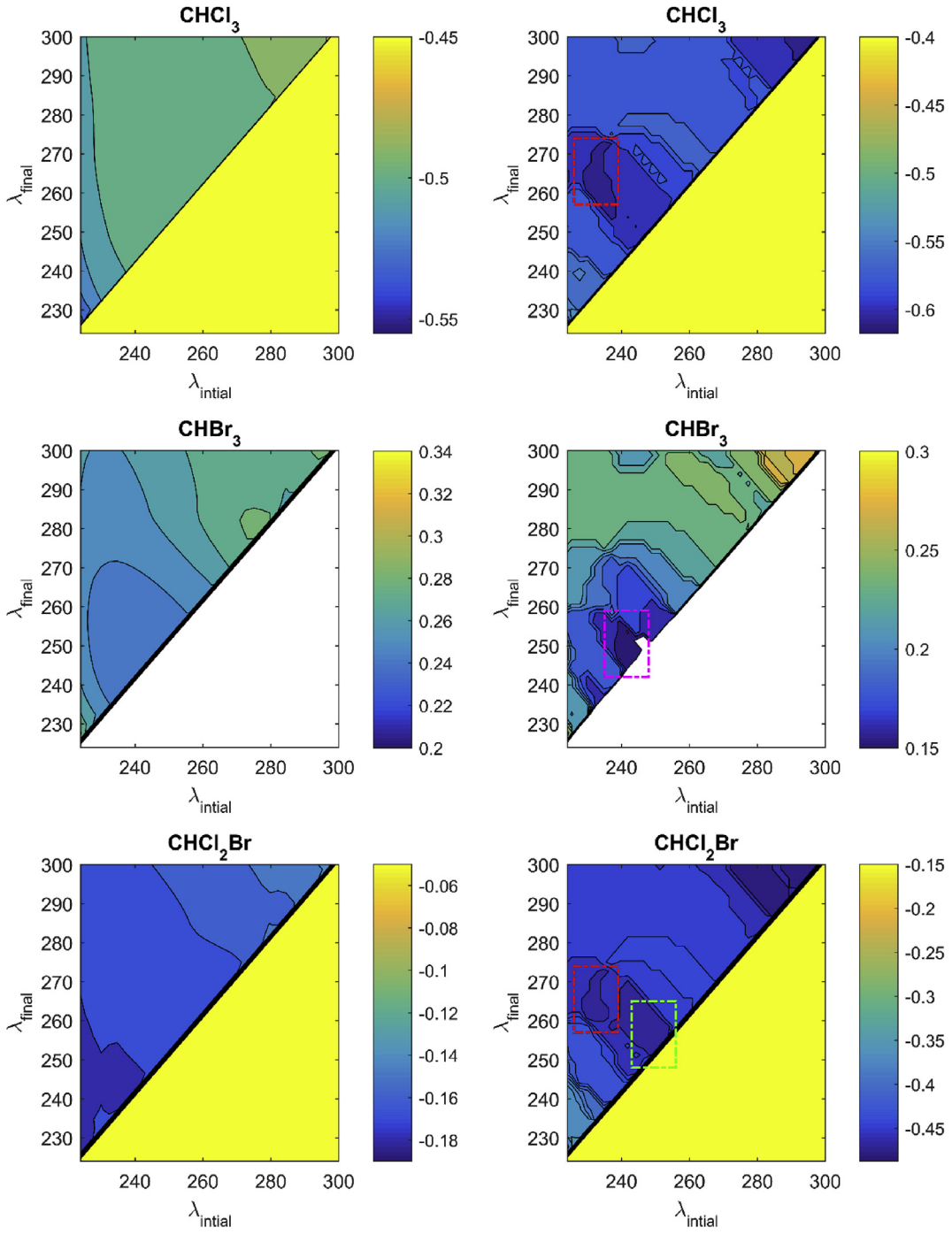

Fig. 7. Pearson and Spearman correlation coefficient evaluated for the integral array described in Section 2.4. Plots on the right describe those evaluated using the Spearman coefficient, and those on the left are evaluated using the Pearson coefficient. The red dashed box represents absorbance moieties at $\lambda_{int} = 226–239$ and $\lambda_{fin} = 257\text{-}273$ (S1), the green dashed box for moieties at $\lambda_{int} = 243–256$ and $\lambda_{fin} = 248\text{-}265$ (S2), and the purple dashed box for moieties at $\lambda_{int} = 235–248$ and $\lambda_{fin} = 242\text{-}259$ (S3). (For interpretation of the references to colour in this figure legend, the reader is referred to the Web version of this article.)

using HPSEC coupled with photodiode array detection; and were used to test their association with common water quality parameters and THM species via correlation coefficients. Samples from DB, MOR, and LET all found a decrease in UVA moieties at an AMW range of 2.2-4 k Da following treatment with SBA resin. It was also found that the presence (or disappearance) of this peak were associated with values for TOC, UVA_{254}, and TTHM4 upon initial observations; thereby identifying components in the range of 2.2-4 k Da as being heavily responsibly for many water parameters of concern for potable water treatment. High correlations were found between TTHM, TOC values and UVA moieties in the 1.6–2.1 k Da range when evaluating Spearman and Pearson correlation coefficients. This was further evident by determining the adjusted R^2 which also showed a strong linear relationship between these variables. This relationship was stronger than that determined between 2.2 k-4k Da, which may be another distinction between FA and HA components of NOM - as both of these AMW ranges were present in the SRNOM chromatogram.

When the correlation coefficients were extended to include individual THM4 species (with the exception of $CHClBr_2$), the associations grew much stronger. Components between 2.2-4 k Da were heavily associated with $CHCl_2Br$ and $CHCl_3$, with medium associations at other AMW and wavelength intervals. $CHBr_3$ was found to show an alternative trend that the chlorinated species, which was found to be due to the removal of bromide by the IX treatment itself, or, the greater formation of brominated-THM species with increased FA character. When investigating the relationship using the Spearman coefficient, coefficients improved for all wavelength intervals tested. This helps to highlight the reactive nature of components between 2.2-4 k Da to the formation of THM species, especially with that of $CHCl_3$ – a species which typically dominates TTHM formation in most potable water supplies.

An array of correlation coefficients based on initial and final wavelengths was utilized to provide a means to pinpoint UV moieties that correspond to surrogate parameters of NOM and THM species. associations based on the Spearman coefficient identified specific regions of interest between UVA_{254}, TTHM, $CHCl_3$, and $CHCl_2Br$ at $\lambda_{int} = 226–239$ and $\lambda_{fin} = 257-273$. These regions specified relate to an assortment of UV moieties that can be used by researchers to better understand the precursor products contributing most to TTHM formation. These ranges can be used to better prepare surrogate compounds in the investigation of the "black-box" phenomenon of the THM reaction pathway. Another region of interest was specific to $CHCl_2Br$ and UVA_{254}, which may lead one to believe these parameters are closely related via an intermediary aromatic byproduct. A better understanding of the HPSEC chromatogram through peak identification and quantification can provide researchers with a more formulated understanding of NOM characterization and additionally THM formation.

Appendix A. Supplementary data

Supplementary data to this article can be found online at https://doi.org/10.1016/j.chemosphere.2019.02.176.

References

Apell, J., Boyer, T., 2010. Combined ion exchange treatment for removal of dissolved organic matter and hardness. Water Res. 44 (8), 2419–2430.

Boyer, T., Singer, P., 2005. Bench-scale testing of a magnetic ion exchange resin for removal of disinfection by-product precursors. Water Res. 39, 1265–1276.

Brezinski, K., Gorczyca, B., 2019. An overview of the uses of high performance size exclusion chromatography (HPSEC) in the characterization of natural organic matter (NOM) in portable water, and ion-exchange applications. Chemosphere 122–139.

Cabaniss, S., Zhou, Q., Maurice, P., Chin, Y., Aiken, G., 2000. A log-normal distribution model for the molecular weight of aquatic fulvic acids. Environ. Sci. Technol. 34, 1103–1109.

Chabalina, L.D., Pastor, M.R., Rico, D.P., 2013. Characterization of soluble and bound EPS obtained from 2 submerged Membr. bioreactors by 3D-EEM and HPSEC. Talanta 115, 706–712.

Chin, Y., Aiken, G., Danielson, K., 1997. Binding of pyrene to aquatic humic substances: the role of molecular weight and aromaticity. Environ. Sci. Technol. 31, 1630.

Chin, Y., Aiken, G., O'Loughlin, E., 1994. Molecular weight, polydispersity, and spectroscopic properties of aquatic humic substances. Environ. Sci. Technol. 28 (11), 1853–1858.

Chow, A., Dahlgren, R., Zhang, Q., Wong, P., 2008. Relationships between specific ultraviolet absorbance and trihalomethane precursors of different carbon sources. Aqua 57, 471–480.

Comstock, S., Boyer, T., Graf, K., 2011. Treatment of nanofiltration and reverse osmosis concentrates: comparison of precipitative softening, coagulation, and anion exchange. Water Res. 45, 4855–4865.

Cory, R., McKnight, D., 2005. Fluorescence spectroscopy reveals ubiquitous presence of oxidized and reduced quinones in dissolved organic matter. Environ. Sci. Technol. 39, 8142–8149.

Drikas, M., Dixon, M., Morran, J., 2011. Long term case study of MIEX pre-treatment in drinking water; understanding NOM removal. Water Res. 45, 1539–1548.

Eszwald, J. a., 2010. Water Quality & Treatment - a handbook on drinking water 6th edition. In: Eszwald, J. (Ed.), Chemical Principles, Source Water Composition, and Watershed Protection. AWWA and McGraw-Hill, New York.

Flowers, R., Singer, P., 2013. Anion exchange resins as a source of nitrosamines and nitrosamine precursors. Environ. Sci. Technol. 47, 7365–7372.

Fuoss, R., Strauss, U., 1948. Electrostatic interaction of polyelectrolytes and simple electrolytes. J. Polym. Sci. 3, 602–603.

Gough, R., Holliman, P., Willis, N., Jones, T., Freeman, C., 2012. Influence of habitat on the quantity and composition of leachable carbon in the O2 horizon: potential implications for potable water treatment. Lake Reservoir Manag. 28 (4), 282–292.

Ha, B., Thirumalai, D., 1992. Conformations of a polyelectrolyte chain. Phys. Rev. 46, R3012 (R).

Health Canada, 2006. Guidelines for Canadian Drinking Water Quality: Guideline Technical Document - Trihalomethanes. Water Quality and Health Bureau, Ottawa.

Helms, J., Stubbins, A., Ritchie, J., Minor, E., Kieber, D., Mopper, K., 2008. Absorption spectral slopes and slope ratios as indicators of molecular weight, source, and photobleaching of chromophoric dissolved organic matter. Limnol. Oceanogr. 53 (3), 955–969.

Her, N., Amy, G., Sohn, J., Gunten, U., 2008. UV absorbance ration index with size exclusion chromatography (URI-SEC) as an NOM property indicator. J. Water Supply Resour. Technol. 57, 35–44.

Hidayah, E., Chou, Y., Yeh, H., 2016. Using HPSEC to identify NOM fraction removal and the correlation with disinfection by-product precursors. Water Sci. Technol. Water Supply 16 (2), 305–313.

Hong, H., Yan, X., Song, X., Qin, Y., Sun, H., Lin, H., Chen, J., Liang, Y., 2017. Bromine incorporation into five DBP classes upon chlorination of water with extremely low SUVA values. Sci. Total Env. 590-591, 720–728.

Hu, C., Zhu, H., Lin, Y., Zhang, T., Zhang, F., Xu, B., 2015. Dissolved organic matter fractions and disinfection by-product formation potential from major raw waters in the water-receiving areas of south-to-north water diversion project, China. Desalination Water Treat. 56 (6), 1689–2697.

Huang, H., Chow, C., Jin, B., 2016. Characterization of dissolved organic matter in stormwater using high-performance size exclusion chromatography. J. Environ. Sci. 41, 236–245.

Huber, S., Balz, A., Abert, M., Pronk, W., 2011. Characterisation of aquatic humic and non-humic matter with size-exclusion chromatography – organic carbon detection – organic nitrogen detection (LC-OCD-OND). Water Res. 45 (2), 879–885.

Jan, J., Breedveld, V., 2008. Microrheological study of polyelectrolyte collapse and reexpansion in the presence of multivalent counterions. Macromolecules 41, 6517–6522.

Jiang, J., Zhang, X., Zhu, X., Li, Y., 2017. Removal of intermediate aromatic halogenated DBPs by activated carbon adsorption: a new approach to controlling halogenated DBPs in chlorinated drinking water. Environ. Sci. Technol. 51 (6), 2017.

Kaewsuk, J., Seo, G., 2011. Verification of NOM removal in MIEX-NF system for advanced water treatment. Separ. Purif. Technol. 80, 11–19.

Karanfil, T., Schlautman, M., Erdogan, I., 2002. Survey of DOC and UV measurement practices with implications for SUVA determination. J. Am. Water Work. 94, 68–80.

Kim, D., Moon, S., Cho, J., 2002. Investigation of the adsoption and transport of natural organic matter (NOM) in ion-exchange Membr.s. Desalination 151, 11–20.

Korshin, G., Chow, C., Fabris, R., Drikas, M., 2009. Adsorbance spectroscopy-based examination of effects of coagulation on the reactivity of fractions of natural organic matter with varying apparent molecular weights. Water Resour. 43, 1541–1548.

Kottisch, V., Gentenkos, D., Fors, B., 2016. "Shaping" the future of molecular weight distributions in anionic Poly.ization. ACS Macro Lett. 5 (7), 796–800.

Lavonen, E., Gonsior, M., Tranvik, L., Schmitt-Kopplin, P., Kohler, S., 2013. Selective chlorination of natural organic matter: identification of previously unknown disinfection byproducts. Environ. Sci. Technol. 47, 2264–2271.

Lee, N., Amy, G., Croué, J., Buisson, H., 2004. Identification and understanding of fouling in low-pressure Membr. (MF/UF) filtration by natural organic matter (NOM). Water Res. 38, 4511–4523.

Lewis, R., van Leeuwen, J., Chow, C., Everson, A., Lewis, D., 2012. Assessment of coagulated and non-coagulated ASB performance used to treat Pinus radiata sulfite pulp and paper mill effluent by resin fractionation and HPSEC techniques. Chem. Eng. J. 213, 109–117.

Liang, L., Singer, P., 2003. Factors influencing the formation and relative distribution of haloacetic acids and trihalomethanes in drinking water. Environ. Sci. Technol. 37, 2920–2928.

Lin, L., Xu, B., Lin, Y.-L., Hu, C.-Y., Ye, T., Zhang, T.-Y., Tian, F.-X., 2014. A comparison of carbonaceous, nitrogenous and iodinated disinfection by-products formation potential in different dissolved organic fractions and their reduction in drinking water treatment processes. Separ. Purif. Technol. 133, 82–90.

Liu, S., Lim, M., Fabris, R., Chow, C., Drikas, M., Amal, R., 2010. Comparison of photolytic degradation of natural organic matter in two Australian surface waters using multiple analytical techniques. Org. Geochem. 41, 124–129.

Mergen, M., Adam, B., Vero, G., Prices, T., Parsons, S., Jefferson, B., Jarvis, P., 2009. Characterization of natural organic matter (NOM) removed by magnetic ion-exchange resin (MIEX Resin). Water Sci. Technol. Water Supply 9 (2), 199–205.

Mergen, M., Jefferson, B., Parsons, S., Jarvis, P., 2008. Magnetic ion-exchange resin treatment: impact of water type and resin use. Water Res. 41, 1977–1988.

Najim, I., Trussel, R., 2001. NDMA formation in water and wastewater. J. Am. Water Work. Assoc. 93, 92–99.

Pan, Y., Zhang, X., 2013. Four groups of new aromatic halogenated disinfection byproducts: effect of bromide concentration on their formation and speciation in chlorinated drinking water. Environ. Sci. Technol. 47 (3), 1265–1273.
Pan, Y., Li, H., Zhang, X., Li, A., 2016. Characterization of natural organic matter in drinking water: sample preparation and analytical approaches. Trends Environ. Anal. Chem. 12, 23–30.
Perminova, I., Frimmel, F., Kovalevskii, D., Abbt-Braun, G., Kudryavtsev, A., 1998. Development of predictive model for calculation of molecular weight of humic substances. Water Res. 32 (3), 872–881.
Phetrak, A., Lohwacharin, J., Takizawa, S., 2016. Analysis of trihalomethane precursor removal from sub-tropical reservoir waters by a magnetic ion exchange resin using a combined method of chloride concentration variation and surrogate organic molecules. Sci. Total Environ. 539, 165–174.
Potter, B., Wimsatt, J., 2005. Method 415.3 - 1. Measurement of Total Organic Carbon, Dissolved Organic Carbon and Specific UV Absorbance at 254 Nm in Source Water and Drinking Water. U.S. Env. Protection Agency, Washington, DC.
Rice, E., Baird, R., Eaton, A., Clesceri, L., 2012. Standard Methods for the Examination of Water and Wastewater. American Public Health Association, American Water Works Association, Water Environment Federation, Denver.
Rodrigues, P., Esteves da Silva, J., Antunes, M., 2007. Factorial analysis of the trihalomethanes formation in water disinfection using chlorine. Anal. Chim. Acta 595, 266–274.
Ruhl, A., Jekel, M., 2012. Elution behaviour of low molecular weight compounds in size exclusion chromatography. J. Water Supply Res. Technol. - Aqua 61, 32–40.
Thurman, E., 1985. Org. Geochem. Of Natural Waters. Springer Netherlands, Houten.
Weishaar, J., Aiken, G., Bergamaschi, B., Fram, M., Fugii, R., Mopper, K., 2003. Evaluation of specific ultraviolet absorbance as an indicator of the chemical composition and reactivity of dissolved organic carbon. Environ. Sci. Technol. 37, 4702–4708.
Whitehead, R., Cole, J., 2006. Different responses to nitrate and nitrite by the model organism Escherichia coli and the human pathogen Neisseria gonorrhoeae. Biochem. Soc. Trans. 34, 111–114.
WHO, 2017. Guidelines for Drinking-Water Quality: Fourth Edition Incorporating the First Addendum. World Health Organization, Geneva: Geneva.
Yan, M., Korsin, G., Wang, D., Cai, Z., 2012. Characterization of dissolved organic matter using high-performance liquid chromatography (HPLC)-size exclusion chromatography (SEC) with a multiple wavelength absorbance detector. Chemosphere 87, 879–885.
Yau, W., Kirkland, J., Bly, D., 1979. Modern Size Exclusion Chromatography. John Wiley and Sons, New York.
Zhai, H., Zhang, X., 2011. Formation and decomposition of new and unknown polar brominated disinfection byproducts during chlorination. Environ. Sci. Technol. 45 (6), 2194–2201.
Zhang, T., Lu, J., Ma, J., Qiang, Z., 2008. Fluorescence spectroscopic characterization of DOM fractions isolated from a filtered river water after ozonation and catalytic ozonation. Chemosphere 71, 911–921.
Zhou, Q., Cabaniss, S., Maurice, P., 2000. Considerations in the use of high-pressure size exclusion chromatography (HPSEC) for determining molecular weights of aquatic humic substances. Water Res. 34, 3505–3514.